Anharmonic Interaction Signals for Acoustic Detection of Analyte

Sourav K Ghosh, Victor P Ostanin, Ashwin A Seshia[*]

University of Cambridge Nanoscience Centre, 11 J J Thomson Avenue,

Cambridge, Cambridgeshire, United Kingdom, CB3 0FF

Abstract

This document describes the derivations of certain important parameters that form the basis of the assumptions used in the models presented in the primary article. This also captures the detailed materials and methods used in the experiments and some additional results. This document is intended not to be read independently but as and when directed from the primary article.

S-I. ESTIMATION OF THE FUNDAMENTAL RESONANT FREQUENCY OF THE PARTICLE-TETHER SYSTEM

The fundamental resonant frequency of particle-tether system is estimated for a SCPM bead and a streptavidin-thiolated-biotin tether. The longitudinal stiffness k_l of a single streptavidin-biotin link in the tether is calculated using the results of the work by Jian *et al.* [1]. From their published graphs, the stiffness at the slow pulling velocity of 1 *μm/s* can be calculated to be around 350 *pN/nm* ($F = 70 pN$ corresponds to $Z_{tip} = 2 A°$). Since the centres of the other three monomers were constrained in their work, which is not the case in reality, the actual stiffness value k_l is lower. In this work, k_l is approximately estimated to be 100 *pN/nm*. This is used to compute the number of streptavidin-biotin links formed between an streptavidin-coated polystyrene bead (SCPM) bead and the surface as follows. Using the Equipartition Theorem, the elastic energy stored in a link with single degree of freedom can be related to the temperature T_a of the system as

$$\frac{1}{2}k_l d^2 = \frac{1}{2}k_b T_a,$$

where d is the elongation of the link and k_b is the Boltzmann constant. Hence,

$$d = \sqrt{\frac{k_b T_a}{k_l}} = 0.204\, nm,$$

assuming $T_a = 300 K$ and $k_l = 100$ *pN/nm*.

Using this value of d, the semi-vertical angle θ of the cone corresponding to the circular area of bond formation, as shown in Fig. S-3, can be computed as

$$\theta = \cos^{-1}\left(1 - \frac{d}{R_b}\right) = 0.691\, \text{deg},$$

where $R_b = 2.8\,\mu m$, for a 5.6 *μm* SCPM bead.
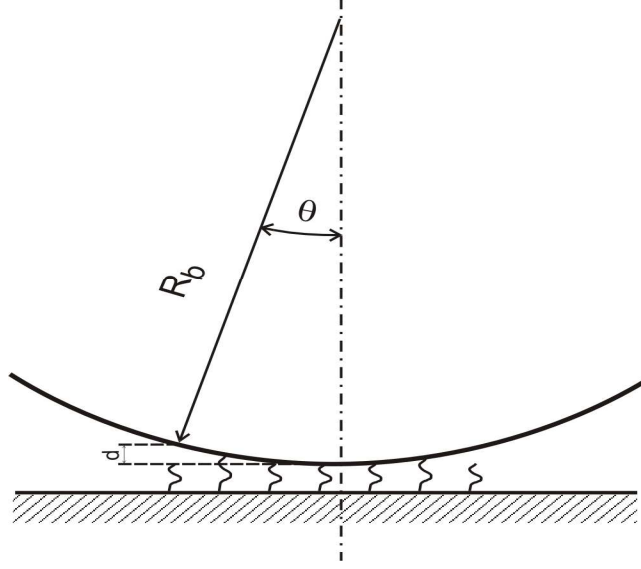
Figure S-1: Calculation of number of links with SCPM bead

The number of links can then be given by

$$n_l = \frac{\pi (R_b \theta)^2}{4\pi R_b^2} n_s \approx 33,$$

where n_s is the number of streptavidin molecules on a 5.6 μm SCPM bead, as obtained from the specifications of Bangs Laboratories, Inc., Fishers, IN, US (n_s = 916,341). The tangential stiffness k_t in the direction perpendicular to the length, i.e. in the direction of drive, can be approximately estimated to be at least one order less i.e. around 10 pN/nm. The fundamental resonant frequency in the tangential direction can then be computed as

$$f_t = \frac{1}{2\pi} \sqrt{\frac{n_l k_t}{m_b}} = 0.302 \, MHz$$

where m_b is the mass of a 5.6 μm SCPM bead assuming the density of polystyrene as 1 gm/cc. Clearly, this is much below the drive frequency, which is usually several MHz; e.g. in the experiments reported here, the drive frequency is 14.3 MHz. So it is assumed in our analytical model that the beads are virtually standing in the direction of drive.

S-II. DERIVATION OF LJ FORCE USED IN THE ANALYTICAL MODEL

A weak electrostatic non-bonded interaction (Van der Waals) is illustrated in the analytical model with a 6-12 Lennard-Jones (LJ) type interaction, which is given by

$$V(r) = 4\varepsilon\left[\left(\frac{\sigma}{r}\right)^{12} - \left(\frac{\sigma}{r}\right)^{6}\right]$$

Here r is the distance between particles, ε is the depth of potential well and σ is the finite distance at which the inter-particle potential is zero. The expression of LJ force can then be given by

$$F(r) = \frac{\partial}{\partial r}V(r) = 24\varepsilon\left[\frac{\sigma^{6}}{r^{7}} - 2\frac{\sigma^{12}}{r^{13}}\right]$$

The tether length l corresponds to r in the above equation. To get $F(l) = 0$ at scaled equilibrium length $l = 1$, we take $\sigma = \dfrac{1}{2^{1/6}}$ units. Hence, the modified LJ force used in this model is as follows.

$$FLJ(l) = 12\varepsilon\left[\frac{1}{l^{7}} - \frac{1}{l^{13}}\right]$$

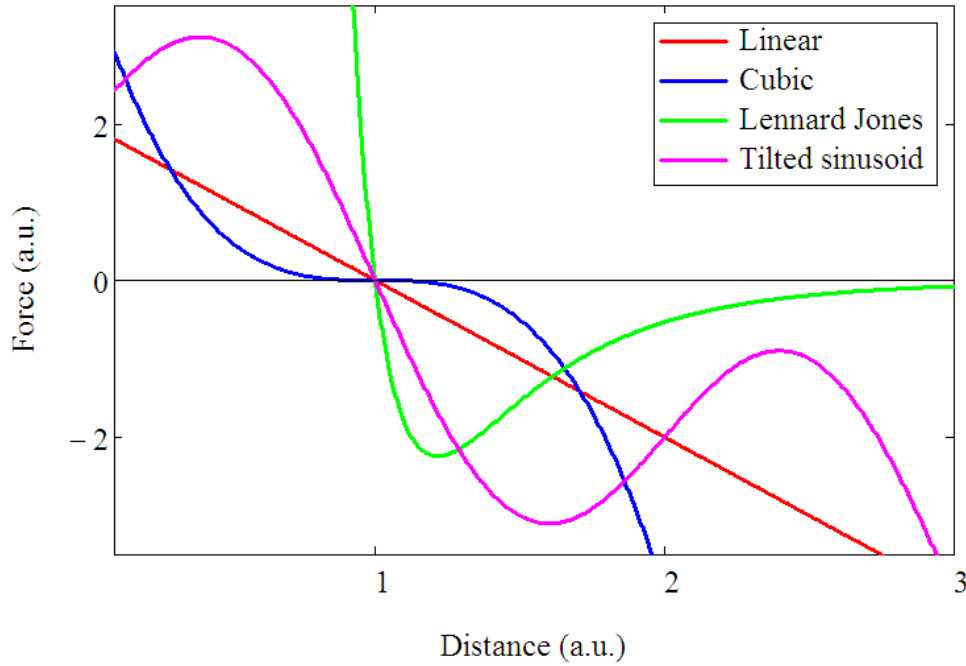The various force functions between the particle and the surface are demonstrated in Fig. S-2.

Figure S-2: Different functions of interaction force vs. tether length used in this model

The equilibrium vertical positions for each of the force functions are demonstrated in Fig. S-3.
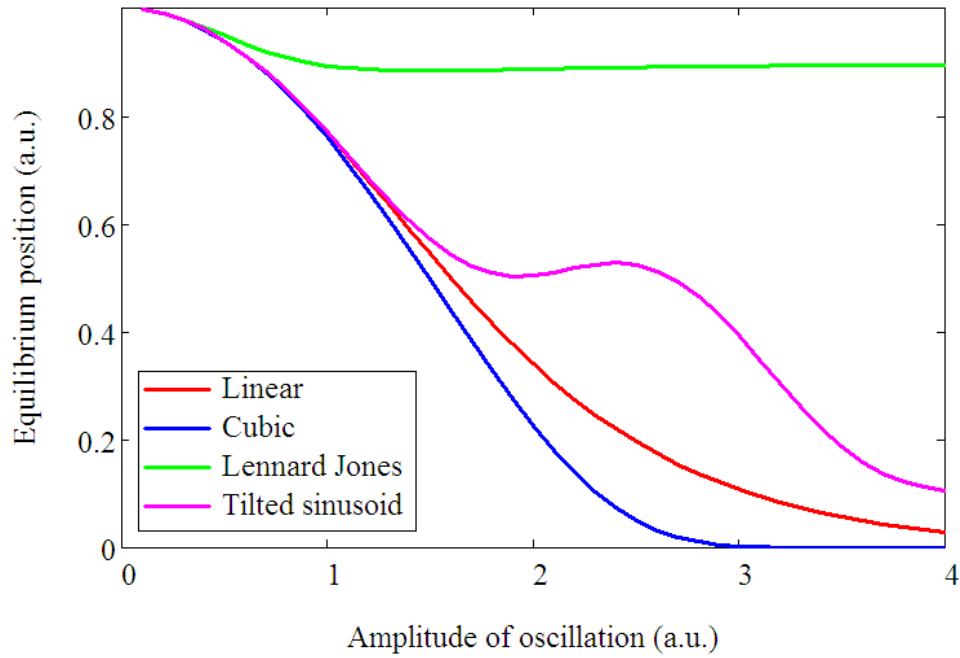
Figure S-3: Vertical position of equilibrium versus amplitude of oscillation

S-III. MATERIALS, METHODS AND RESULTS

A. Instrumentation

As shown in Fig. S-4, a 33220A Agilent function generator was used to generate a 14.3 *MHz* AC signal, linearly rising in amplitude from 0.035 *V* rms to 3.5 *V* rms. This signal was amplified and fed through a low pass filter to remove undesired harmonic distortions to act as the input drive signal. The transduced output signal was received by an SR844 lock-in amplifier (Stanford Research Systems) that recorded the complex (amplitude and phase) 3F signal. A passive frequency tripler was used to generate the reference signal for the lock-in. Additionally, two quadrature receivers were employed to detect the complex 1F voltage and the quartz output current.

B. Quartz Crystal Resonators

The quartz crystals used were 8 *mm* in diameter and 112 *μm* in thickness with fundamental resonant frequency of 14.3 *MHz* (Lap-Tech Inc., Bowmanville, Ontario, Canada). They were made from optically polished AT-cut (temperature-compensated) quartz, cut at an angle of 3° to

the crystal optical axis. The crystals had excellent frequency stability with temperature, staying within less than 5 *ppm* shift between 0° and 60° *C*, with an inflection temperature of 25° *C*. The quartz substrate was sandwiched between evaporated layers of gold keyhole-styled electrodes of 165 *nm* thickness, and 6 *mm* and 4 *mm* diameters respectively. There was an adhesion layer of 5 *nm* of chromium between the quartz and the gold layer.

C. Preparation of the Biological Interface

The quartz crystals were washed in acetone and isopropanol (IPA) and treated in Argon plasma in a Barrel Etcher at 250 *W* for 20 *s* to remove all organic and inorganic contaminants. The cleaned crystals were immediately immersed in a 1 *mM* ethanolic solution of thiol and left overnight for a stable formation of self-assembled monolayer (SAM). For preparation of non-specific sensing platforms for SCPM beads, OH-PEG thiol (HS-$(CH_2)_{11}$-$(EG)_3$-OH, TH 002-02, Prochimia, Sopot, Poland) was used, whereas for specific ones, a 3:1 (by volume) mixture of OH-PEG and Biotin thiol (HS-$(CH_2)_{11}$-$(EG)_3$-Biotin, TH 012-01) was used to produce a mixed SAM. On the following day, the unbound thiols were washed thoroughly, first with ultra pure absolute ethanol and then with Milli-Q water (Millipore Corp.). The sensors were then placed in wells of 100 *μL* solution of 5.6 *μm* SCPM beads (Bangs Laboratories, Inc., Fishers, IN, US) in Milli-Q water for 1 *hr*. The streptavidin of the beads bound specifically to the biotin terminals of the mixed SAM in specific sensors and remained physisorbed on the non-specific sensors. The concentration of aqueous solution of SCPM was varied to get different numbers of beads on the surface. For specific sensors, thorough washing with Milli-Q water was done thoroughly to remove all unbound beads.
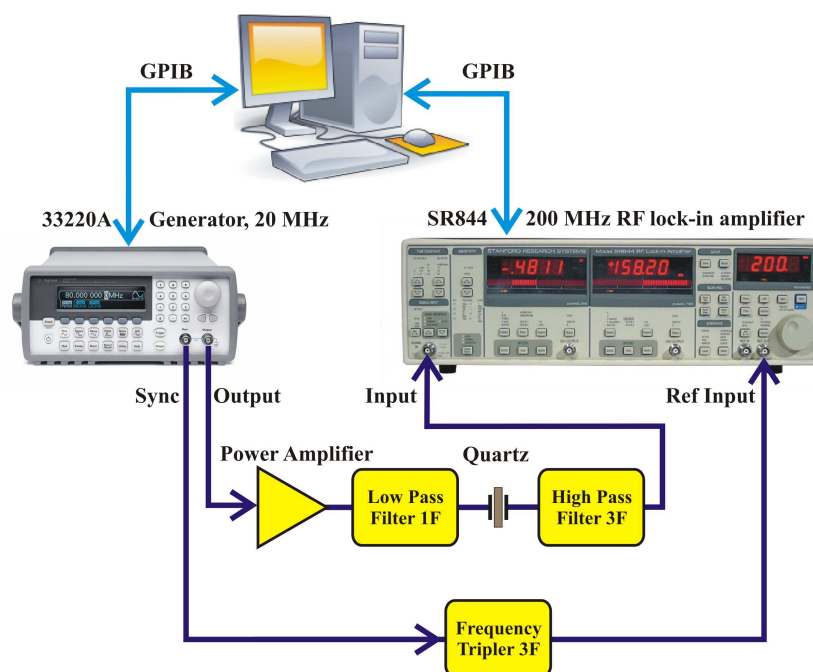
Figure S-4: Schematics of instrumentation

C. Results

Fig. S-5 shows the reproducibility of the successive scans with chemisorbed beads, demonstrating that the measurements using this method are repeatable.
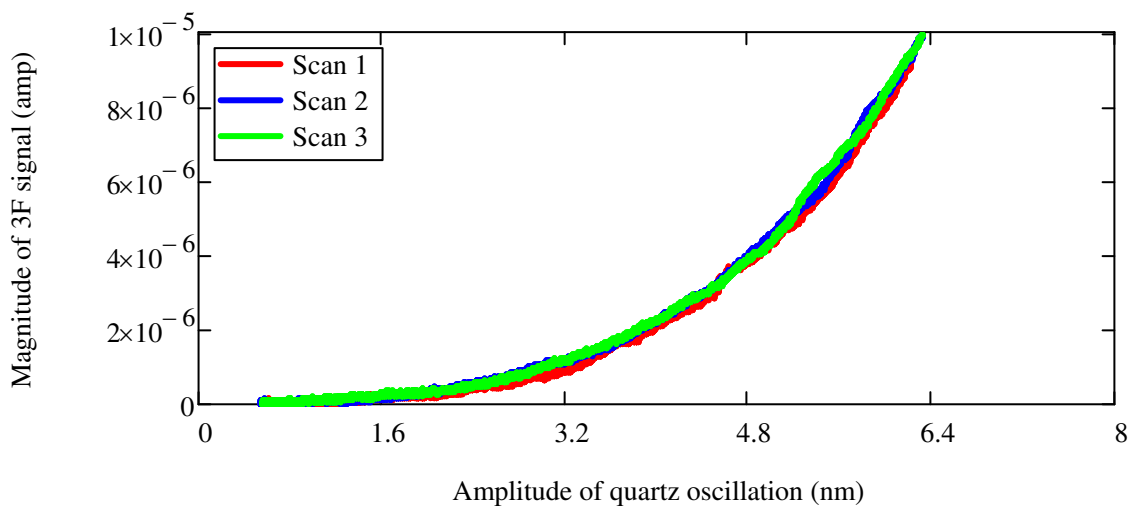

Figure S-5: 3F signal from three scans of a sensor with chemisorbed beads

Fig. S-6 illustrates through linear regression that the 3F signal from a chemisorbed sensor is a cubic function of the oscillation amplitude of the sensor. Hence, if the sensor is calibrated for a

known concentration of target species, the unknown concentration in an analyte can be determined from the ratio of gradient of this linear fit.
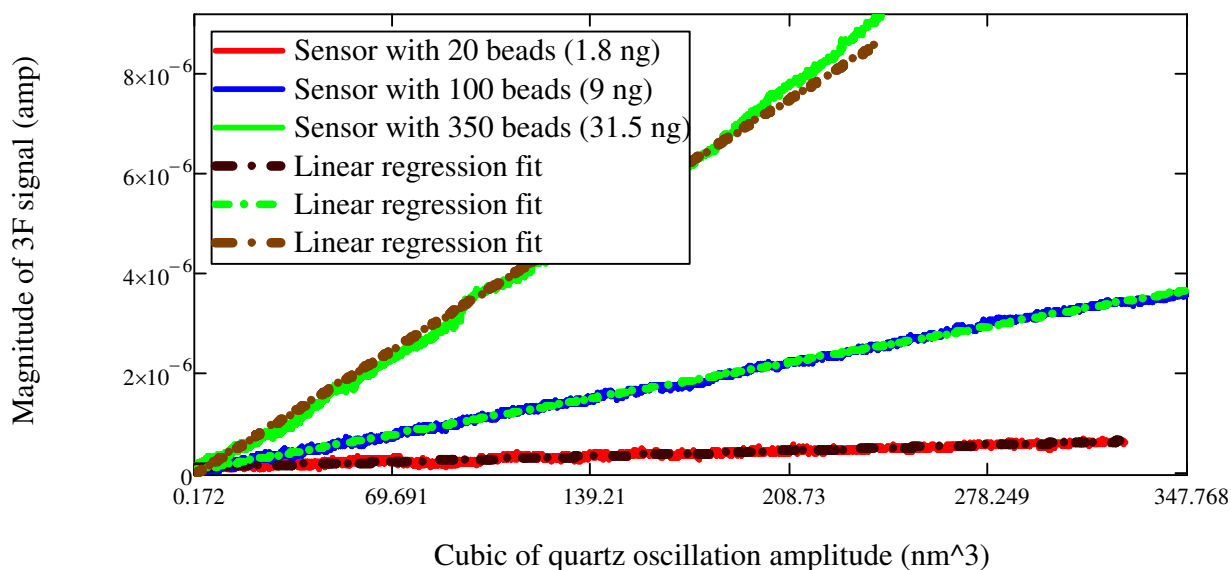

Figure S-6: The 3F signal is a cubic function of oscillation amplitude for all chemisorbed sensors

Fig. S-7 shows the shape of the potential used in the modelling of physisorbed interaction, with the axes units along the surface representing 0.01 nm. The width of potential is equal to the lattice period, assuming point contact of the bead with a perfect Au(111) surface.
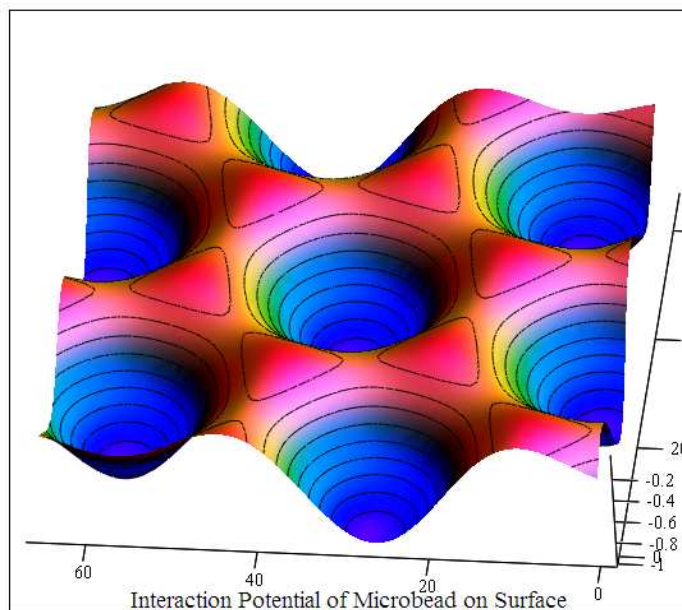
Figure S-7: Interaction potential of microbead on thiolated Au(111) surface

Fig. S-8 shows the force along the tether and the stiffness per bond assumed in the modelling of chemisorbed interaction against the displacement in extension and compression.
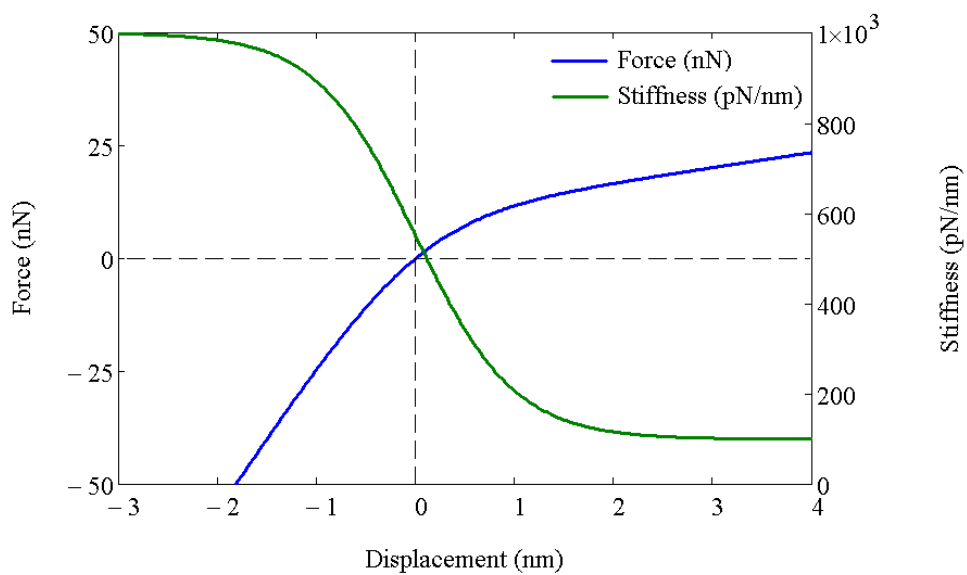

Figure S-8: Force along a tether and stiffness vs. displacement in compression and extension

References

(1)   Jian, Z.; Luzheng, Z.; Yongsheng, L.; Heng-Kwong, T.; Sheng, Y. J.; Shaoyi, J. *Journal of Chemical Physics* **2006,** *125,* **104905-104901-104907.**